

Generating and Stabilizing Co(I) in a Nanocage Environment

Jingmei Shen,[†] Mayfair C. Kung,^{*,†} Zhongliang Shen,[†] Zhen Wang,[†] William A. Gunderson,[‡] Brian M. Hoffman,[‡] and Harold H. Kung^{*,†}

[†]Department of Chemical & Biological Engineering, [‡]Department of Chemistry, Northwestern University, 2145 Sheridan Road, Evanston, Illinois 60208, United States

S Supporting Information

ABSTRACT: A discrete nanocage of core–shell design, in which carboxylic acid groups were tethered to the core and silanol to the shell interior, was found to react with $\text{Co}_2(\text{CO})_8$ to form and stabilize a $\text{Co(I)}\text{--CO}$ species. The singular CO stretching band of this new Co species at 1958 cm^{-1} and its magnetic susceptibility were consistent with Co(I) compounds. When exposed to O_2 , it transformed from an EPR inactive to an EPR active species indicative of oxidation of Co(I) to Co(II) with the formation of H_2O_2 . It could be oxidized also by organoazide or water. Its residence in the nanocage interior was confirmed by size selectivity in the oxidation process and the fact that the entrapped Co species could not be accessed by an electrode.

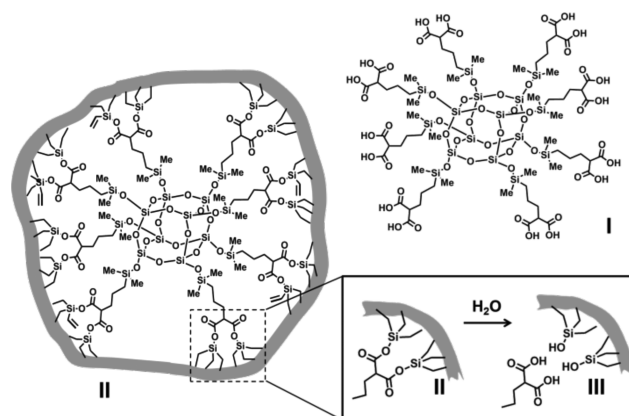
A number of unusual properties of discrete nanocages have emerged since the discovery of carcerand and the recognition of restricted rotational and translational motion for the entrapped molecule.^{1,2} By offering an environment in the interior that differs from the surrounding liquid, nanocages have demonstrated the ability to stabilize ionic reaction intermediates³ and moisture sensitive materials such as phosphorus⁴ and alter molecular conformation,⁵ reaction regioselectivity,^{6,7} reaction rates as well as extent of sequential reaction,⁸ and protonation affinity.⁹ They have also found applications in targeted drug delivery.^{10–12} It is anticipated that new chemical properties would develop as the nanocage design becomes more complex and its functionality more versatile.

Recently, our group has explored creating bifunctional nanocages of a core–shell design, in which the core and the shell interior harbor different functionalities. By linking the core to the shell with a silyl ester bond during synthesis, subsequent hydrolytic cleavage would generate a carboxylic acid on the core and a silanol on the shell. This is a structure that has a hydrophilic interior and a hydrophobic exterior. Thus, it is able to trap and stabilize metal ions in an aprotic solvent.¹³ Because of steric crowding, the motion of the limited number of carboxylic acid groups in the structure is restricted, which could create a situation where a metal complex entering the nanocage can access and react with only a small number of carboxylic acid groups and lead to stabilization of unusual metal complexes. Indeed, it was reported that a stable Zn(I) species could be formed in a microporous crystalline silicoaluminophosphate (SAPO-CHA) by reaction of the vapor of a Zn^0 compound with an isolated H^+ inside a pore,¹⁴ and the resulting Zn -zeolite demonstrated interesting chemical properties such as formation

of acetic acid from methane and low-temperature CO oxidation.^{15,16} This approach to generate an uncommon oxidation state is atypical. In organometallic complexes, manipulating steric and electronic properties of ligands, such as cyclopentadiene, phosphine, imine, guanidine, and carbene, is the usual method to form complexes with the metal in relatively rare and low formal oxidation states, such as complexes of Cr(I) ,^{17–20} Fe(I) ,^{21,22} Co(I) ,^{23–27} and main group elements.²⁸

We report here the formation and stabilization of Co(I) in a discrete molecular, bifunctional, core–shell nanocage by solution chemistry. The nanocage was derived from a nanosphere II, which was formed starting with a malonic acid functionalized spherosilicate core I that was converted to a vinyl-functionalized spherosilicate by reaction with trivinylchlorosilane. Subsequent cross-linking the vinyl groups with 1,4-bis(dimethylsilyl)benzene via hydrosilylation created a porous carbosilane shell (Scheme 1) as previously described.¹³ These silyl ester bonds were easily hydrolyzed, e.g., by dispersing $6.7 \times 10^{-3}\text{ mmol}$ of II in 10 mL of toluene premixed with a stoichiometric amount of water (0.01 M) and stirring at $100\text{ }^\circ\text{C}$ for 24 h. The hydrolysis resulted in carboxylic

Scheme 1. Spherosilicate Core I with 16 Peripheral Acids from Which Silyl Ester Bonds Were Formed, Nanosphere II Formed by Shell Cross-Linking Hydrosilylation of the Peripheral Vinyl Groups with 1,4-Bis-dimethylsilylbenzene^a



^aInset shows hydrolytic cleavage of silyl ester bonds to form functionalized nanocage III.

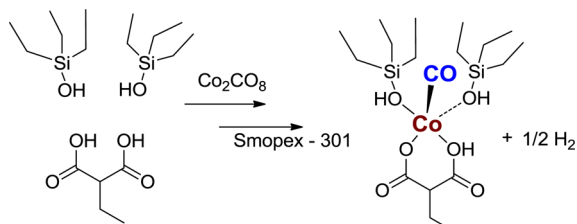
Received: December 6, 2013

Published: March 27, 2014

acid and silanol pairs located inside nanocage **III** (Scheme 1, inset) that can be used to anchor metal cations in the cage interior. Nearly complete hydrolysis of the silyl ester bond was achieved by using a slight excess of water (~ 24 equiv; 1 equiv is 1 mol/mol nanocage). The silanol formed could be detected in ^1H NMR, and the carboxylic acid appeared as a small splitting of the ν_{CO} stretch in the IR spectrum (Figures S1 and S2). These were the only perceptible spectroscopic changes observed, indicating that the rest of the core-shell structure remained intact. However, the width of the ^1H NMR peaks and the overlap of the carbonyl of the silyl ester and carboxylic acid peaks in the IR spectrum prevented quantification of the extent of hydrolysis.

Transformation of **III** into its metalated form Co@III was achieved by reaction with $\text{Co}_2(\text{CO})_8$ followed by purification to remove excess $\text{Co}_2(\text{CO})_8$ (Scheme 2). Analysis by inductively

Scheme 2. Preparative-Scale Reaction and Purification To Form Co@III



coupled plasma indicated that there were ~ 4 Co per nanocage at saturation in Co@III (M.W. **III** $\sim 7900/\text{g}$). The nature of the encapsulated Co species was characterized by FTIR, cyclic voltammetry, EPR, and magnetization. Changes in the FTIR spectra of a solution of 6.7×10^{-4} M **III** in dried toluene containing various amounts of $\text{Co}_2(\text{CO})_8$ are shown in Figure 1. The spectrum for 1 equiv of $\text{Co}_2(\text{CO})_8$ with **III** (curve b) showed the absence of the characteristic, intense absorption features of $\text{Co}_2(\text{CO})_8$ at $2076\text{--}2050\text{ cm}^{-1}$ (terminal carbonyls) or doublet at $1868/1858\text{ cm}^{-1}$ (bridging carbonyls).^{29,30} Instead, a single CO stretch at 1958 cm^{-1} appeared, together with a broad carboxylate band at $\sim 1589\text{ cm}^{-1}$ that overlapped with the slightly diminished carbonyl stretch of the carboxylic

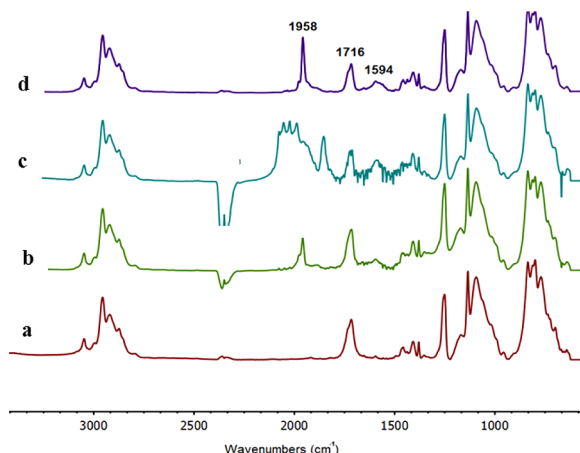


Figure 1. IR spectra of (a) **III**, (b) **III** + 1 equiv of $\text{Co}_2(\text{CO})_8$ after 34 h at rt; (c) **III** + 12 equiv of $\text{Co}_2(\text{CO})_8$; (d) Co@III which is sample c after removal of unreacted $\text{Co}_2(\text{CO})_8$ with Smopex-301 at 50°C in 4 h.

acid of **III**. After adding a total of 12 equiv of $\text{Co}_2(\text{CO})_8$, the carboxylate band intensity increased further, suggesting that each nanocage reacted with more than one $\text{Co}_2(\text{CO})_8$ (curve c). Peaks characteristic of unreacted $\text{Co}_2(\text{CO})_8$ were also present. After removing the unreacted $\text{Co}_2(\text{CO})_8$, the IR spectrum of the resulting clear orange solution of Co@III (curve d) displayed a sharp 1958 cm^{-1} carbonyl peak, peaks at 1716 cm^{-1} (carboxylic acid) and 1594 cm^{-1} (carboxylate), and those associated with the rest of the nanocage. It is worthy to note that, without hydrolyzing the silyl ester bond, the nanosphere **II** did not react with $\text{Co}_2(\text{CO})_8$, as monitored by FTIR (Figure S4). In the literature, the carbonyl peak at 1958 cm^{-1} has been assigned to a Co(I) species.^{25,31,32}

The only change in the ^1H NMR spectrum after reacting **III** with $\text{Co}_2(\text{CO})_8$ was the splitting of the broad, unresolved peak of the phenyl proton of the cage wall ($7.3\text{--}7.7$ ppm) (Figure S5), suggesting interaction of the entrapped Co with the carbosilane shell and their close proximity. Cyclic voltammetry of a THF solution of Co@III was used to determine whether the Co species were located inside the cage or on the outside wall. The CV curve of $\text{Co}_2(\text{CO})_8$ in THF showed redox peaks between -2 and 1 V vs SCE from the $\text{Co}^{\text{I}}/\text{Co}^0$ couple,³³ together with those of the internal standard ferrocene at $0.25\text{--}0.75$ V. The redox peaks for Co were absent for the solution of Co@III , indicating that the Co species were inside the cage and not accessible to the electrode (Figure S6).

The number of CO ligands per Co was determined by thermally decomposing the Co species in Co@III at 80°C and quantifying the CO released. The average stoichiometry was 1 CO per Co (Supporting Information (SI) section VI). The decomposition caused the disappearance of the 1958 cm^{-1} carbonyl peak.

The EPR spectra of Co@III before and after exposure to O_2 (Figure 2) supports the assignment of an initial state of Co(I).

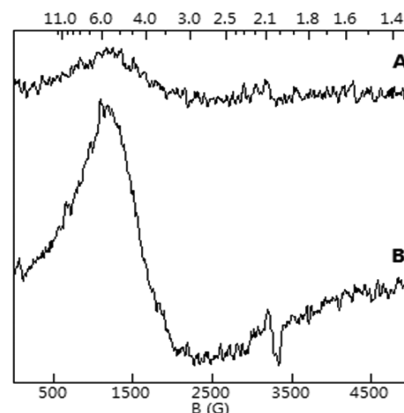


Figure 2. EPR spectra of (A) Co@III and (B) Co@III after 90 min exposure to O_2 . Spectral conditions: microwave frequency = 9.36 GHz , microwave attenuation = 20 dB , modulation amplitude = 13.2 G , modulation frequency = 100 kHz , $T = 7\text{ K}$.

The spectrum of Co@III showed a small signal at $g = 4.0$ from high-spin ($S = 3/2$) Co(II). Quantitation indicated that this sample contained $\sim 0.1\text{ mM}$ of Co(II), accounting for $\sim 10\%$ of the total Co in the sample as prepared, which can be attributed to oxidation during sample preparation. After exposure to O_2 for 90 min the solution changed color from orange to blue-purple. The EPR spectrum showed a corresponding increase in the signal intensity at $g = 4.0$, the signal now accounting for

70% of the Co in the sample. This oxidation of Co(I) to Co(II) was accompanied by the disappearance of the 1958 cm^{-1} band in the IR, although the rest of the spectrum remained unchanged, indicating that the nanocage structure was stable to oxidation (Figure S12). This oxidized species is labeled $\text{Co}_{(\text{ox})}@\text{III}$ (MW = 8248 g/mol).

The magnetic susceptibility of $\text{Co}@\text{III}$ and $\text{Co}_{(\text{ox})}@\text{III}$ were measured in Ar over the range 5–300 K (Figure 3). Both

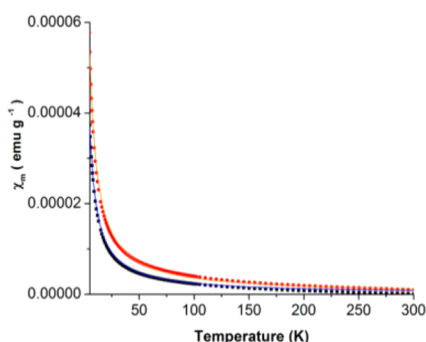


Figure 3. Temperature dependence of mass magnetic susceptibility of $\text{Co}@\text{III}$ (black squares) and $\text{Co}_{(\text{ox})}@\text{III}$ (red dots). The lines are fitting curves.

samples were paramagnetic, and the magnetization followed the Curie–Weiss law.³⁴ From the molar magnetic susceptibility, and assuming that all cobalt centers are independent and homogeneously dispersed in the nanocage, a room temperature effective magnetic moment of $3.55\ \mu_{\text{B}}$ was calculated for $\text{Co}@\text{III}$, which exceeded the expected spin-only value of $2.83\ \mu_{\text{B}}$ for a high-spin d_8 ($S = 1$) system, but was comparable to reported values of other cobalt(I) complexes.^{25,35} Such a difference has been attributed to a substantial orbital angular momentum contribution from the cobalt ion. The $\text{Co}(\text{II})$ species in $\text{Co}_{(\text{ox})}@\text{III}$ was in a $3d^7$ high-spin ($S = 3/2$) state, and its room temperature effective magnetic moment of $5.0\ \mu_{\text{B}}$ was within the range observed for high-spin cobalt(II) complexes with pseudotetrahedral or lower symmetry and suggestive of a quartet magnetic ground state.^{25,36}

The UV–vis spectrum of $\text{Co}@\text{III}$ in toluene showed a very intense metal-to-ligand charge transfer band at 396 nm ($\epsilon = 6.27 \times 10^5\ \text{M}^{-1}\cdot\text{cm}^{-1}$), whereas $\text{Co}_2(\text{CO})_8$ showed absorption at 350 and 280 nm (Figure S10a and c). Upon exposure to O_2 , the absorbance at 396 nm decreased with a pseudo-first-order rate constant of $0.014\ \text{min}^{-1}$ (Figure S10b), and two weak broad bands at 530 nm ($\epsilon = 1045\ \text{M}^{-1}\cdot\text{cm}^{-1}$) and 589 nm ($\epsilon = 1134\ \text{M}^{-1}\cdot\text{cm}^{-1}$) appeared that were indicative of d–d transitions of high-spin $\text{Co}(\text{II})$ (Figure S10c). These spectroscopic changes were visible, as the solution changed from orange to pale blue-purple, corresponding to that seen upon oxygenation of the concentrated EPR sample, as described above.

The product of the reaction of $\text{Co}@\text{III}$ with O_2 was extracted with water and analyzed for H_2O_2 by titration with potassium titanium oxalate (see SI). For a reaction that started with $4 \times 10^{-4}\ \text{mmol}$ of Co, $1.18 \times 10^{-4}\ \text{mmol}$ of H_2O_2 was detected in the aqueous phase, which corresponded to a 59% yield. Trace amounts of benzyl aldehyde and benzyl alcohol were detected by GC/MS in the toluene phase. With handling losses considered, the reduction of O_2 by $\text{Co}@\text{III}$ and hydrolysis to form H_2O_2 appeared to be nearly quantitative.

$\text{Co}@\text{III}$ can be oxidized by organoazide also, and the size selectivity of **III** can be demonstrated by using different organoazides. Two azides of different molecular sizes, phenyl and adamantyl, were tested by adding 1 equiv of oxidant to $\text{Co}@\text{III}$ in toluene ($6.27 \times 10^{-4}\ \text{M}$) and following the reaction with UV spectroscopy (Figure S17). In both cases, the orange solution became pale yellow at the end of the reaction, and the 396 nm band disappeared. The change of color was complete within 2 h for phenyl azide, but took about 12 h for adamantyl azide. Thus, the smaller phenyl azide entered the nanocage much faster than adamantyl azide and further supported the interior location of Co. For both reactions, EPR analyses of the product solution could not detect any signal, and the high reactivity of the nanocage prevented useful analysis by mass spectroscopy. The results from UV–vis spectroscopy and EPR, and the fact that the color remained pale yellow after exposure to air, suggested that the Co(I) in $\text{Co}@\text{III}$ was oxidized to a Co(III) species. At present, it is not known whether the product is a Co-imido species or Co coordinated to more than one organoazide. In the literature, there are examples of organoazide oxidation of Co(I) to cobalt(III) imido complexes.^{35,37,38} H_2O was also effective in oxidizing $\text{Co}@\text{III}$.

In order to confirm the relevance of the nanocage environment in this process, the reaction of $\text{Co}_2(\text{CO})_8$ with the spherosilicate template **I** in toluene was examined. **I** possesses 16 carboxylic acid groups on the periphery. This reaction resulted in a pink precipitate of rather uniform, spherical globules about 200 nm in diameter (Figure S13). XPS of the precipitate indicated formation of Co(II) (Figure S16). Apparently, $\text{Co}_2(\text{CO})_8$ was oxidized by reaction with the carboxylic acids to form a network of spherosilicate carboxylate cross-linked with Co(II).

Thus, we have demonstrated that a nanocage with a core–shell structure, containing a prescribed number of common functional groups and restricted space for movement of complexes, can be used to generate and stabilize metal complexes of an uncommon oxidation state with a high degree of uniformity. In this example, this is achieved by limiting the number of carboxylic acid groups accessible to each Co carbonyl complex. The concept is general, and the approach has the potential to greatly expand the tools for stabilizing low-valent metal ions, in addition to the standard approach of manipulating the properties of ligands that include Cp, phosphines, and others. When coupled with the properties of hydrophilic interior and hydrophobic exterior, these nanocages can be used with other metal complexes of a variety of properties, creating opportunities to explore new metal complexes of uncommon oxidation states.

■ ASSOCIATED CONTENT

● Supporting Information

Experimental details, IR, UV–vis, NMR, cyclic voltammetry, EPR spectroscopy, and magnetism results. This material is available free of charge via the Internet at <http://pubs.acs.org>.

■ AUTHOR INFORMATION

Corresponding Authors

m-kung@northwestern.edu

hkung@northwestern.edu

Notes

The authors declare no competing financial interest.

■ ACKNOWLEDGMENTS

J.S., Z.W., and H.H.K. were supported by U.S. DOE Grant (DE-FG02-01ER15184). Z.S. and M.C.K. were supported by the Institute for Atom-efficient Chemical Transformations (IACT), an Energy Frontier Research Center funded by the U.S. DOE, Office of Science, Office of Basic Energy Sciences. W.A.G. and B.M.H. (EPR data) were supported by the NIH (Grant NH13531). We acknowledge SQUID measurements by Dr. O. Chernyashvskyy at Northwestern's magnetic and physical properties measurement facility supported by the NSF, UV-vis facility of the Keck Biophysics Facility, and Dr. M. Katz and Prof. J. Hupp for use of the electrochemical scanning microscope, all at Northwestern University.

■ REFERENCES

- (1) Cram, D. J. *Nature* **1992**, 356, 29.
- (2) Sherman, J. C. *Tetrahedron* **1995**, 51, 3395.
- (3) Pluth, M. D.; Begman, R. G.; Raymond, K. N. *Science* **2007**, 316, 85.
- (4) Mal, P.; Breiner, B.; Rissanen, K.; Nitschke, J. R. *Science* **2009**, 324, 1697.
- (5) Trembleau, L.; Rebek, J., Jr. *Science* **2003**, 301, 1219.
- (6) Yoshizawa, M.; Tamaru, M.; Fujita, M. *Science* **2006**, 312, 251.
- (7) Kuil, M.; Soltner, T.; van Leeuwen, P. W. N. M.; Reek, J. N. H. *J. Am. Chem. Soc.* **2006**, 128, 11344.
- (8) Suh, Y.-W.; Kung, M. C.; Wang, Y.; Kung, H. H. *J. Am. Chem. Soc.* **2006**, 128, 2776.
- (9) Henao, J. D.; Suh, Y.-W.; Lee, J.-K.; Kung, M. C.; Kung, H. H. *J. Am. Chem. Soc.* **2008**, 130, 16142.
- (10) Chen, J.; Yang, M.; Zhang, Q.; Cho, E. C.; Cobley, C. M.; Kim, C.; Glaus, C.; Wang, L. V.; Welch, M. J.; Xia, Y. *Adv. Funct. Mater.* **2010**, 20, 3684.
- (11) Skrabalak, S. E.; Chen, J.; Sun, Y.; Lu, X.; Au, L.; Cobley, C. M.; Xia, Y. *Acc. Chem. Res.* **2008**, 41, 1587.
- (12) Xia, Y.; Li, W.; Cobley, C. M.; Chen, J.; Xia, X.; Zhang, Q.; Yang, M.; Cho, E. C.; Brown, P. K. *Acc. Chem. Res.* **2011**, 44, 914.
- (13) Shen, Z.; Kim, J.; Shen, J.; Downing, C. M.; Lee, S.; Kung, H. H.; Kung, M. C. *Chem. Commun.* **2013**, 49, 3357.
- (14) Tian, Y.; Li, G.-D.; Chen, J.-S. *J. Am. Chem. Soc.* **2003**, 125, 6622.
- (15) Wang, X.; Qi, G.; Xu, J.; Li, B.; Wang, C.; Deng, F. *Angew. Chem., Int. Ed.* **2012**, 51, 3850.
- (16) Qi, G.; Xu, J.; Su, J.; Chen, J.; Wang, X.; Deng, F. *J. Am. Chem. Soc.* **2013**, 135, 6762.
- (17) Shen, J.; Yap, G. P.; Werner, J. P.; Theopold, K. H. *Chem. Commun.* **2011**, 47, 12191.
- (18) Monillas, W. H.; Yap, G. P.; Theopold, K. H. *Angew. Chem., Int. Ed.* **2007**, 46, 6692.
- (19) Kreisel, K. A.; Yap, G. P.; Dmitrenko, O.; Landis, C. R.; Theopold, K. H. *J. Am. Chem. Soc.* **2007**, 129, 14162.
- (20) Monillas, W. H.; Yap, G. P.; MacAdams, L. A.; Theopold, K. H. *J. Am. Chem. Soc.* **2007**, 129, 8090.
- (21) Holland, P. L.; Cundari, T. R.; Perez, L. L.; Eckert, N. A.; Lachicotte, R. J. *J. Am. Chem. Soc.* **2002**, 124, 14416.
- (22) Thomas, C. M.; Liu, T.; Hall, M. B.; Darensbourg, M. Y. *Inorg. Chem.* **2008**, 47, 7009.
- (23) Jones, C.; Schulten, C.; Rose, R. P.; Stasch, A.; Aldridge, S.; Woodul, W. D.; Murray, K. S.; Moubaraki, B.; Brynda, M.; La Macchia, G.; Gagliardi, L. *Angew. Chem., Int. Ed.* **2009**, 48, 7406.
- (24) Dugan, T. R.; Sun, X.; Rybak-Akimova, E. V.; Olatunji-Ojo, O.; Cundari, T. R.; Holland, P. L. *J. Am. Chem. Soc.* **2011**, 133, 12418.
- (25) Hu, X.; Castro-Rodriguez, I.; Meyer, K. J. *J. Am. Chem. Soc.* **2004**, 126, 13464.
- (26) Egan, J. W.; Haggerty, B. S.; Rheingold, A. L.; Sendlinger, S. C.; Theopold, K. H. *J. Am. Chem. Soc.* **1990**, 112, 2445.
- (27) Lin, T.-P.; Peters, J. C. *J. Am. Chem. Soc.* **2013**, 135, 15310.
- (28) Schulz, S. *Chem.—Eur. J.* **2010**, 16, 6416.
- (29) Kurhinen, M.; Pakkanen, T. A. *Langmuir* **1998**, 14, 6907.
- (30) Tannenbaum, R. *Inorg. Chim. Acta* **1994**, 227, 233.
- (31) Detrich, J. L.; Konečný, R.; Vetter, W. M.; Doren, D.; Rheingold, A. L.; Theopold, K. H. *J. Am. Chem. Soc.* **1996**, 118, 1703.
- (32) Pollard, M. J.; Weinstock, B. A.; Bitterwolf, T. E.; Griffiths, P. R.; Piers Newbery, A.; Paine Iii, J. B. *J. Catal.* **2008**, 254, 218.
- (33) Connelly, N. G.; Geiger, W. E. *Chem. Rev.* **1996**, 96, 877.
- (34) Jolly, W. L. *The Synthesis and Characterization of Inorganic Compounds*; Prentice Hall, Inc.: NJ, 1970.
- (35) Thyagarajan, S.; Shay, D. T.; Incarvito, C. D.; Rheingold, A. L.; Theopold, K. H. *J. Am. Chem. Soc.* **2003**, 125, 4440.
- (36) Boudreaux, E. A. M. L. N. *Theory and Applications of Molecular Paramagnetism*; Wiley: New York, 1976.
- (37) Jenkins, D. M.; Betley, T. A.; Peters, J. C. *J. Am. Chem. Soc.* **2002**, 124, 11238.
- (38) Saouma, C. T.; Peters, J. C. *Coord. Chem. Rev.* **2011**, 255, 920.